

[11] Research of sparse representation method for ringing suppression

A.V. Umnov¹, A.S. Krylov²

¹National Research University Higher School of Economics, Moscow, Russia,

²Lomonosov Moscow State University, Moscow, Russia



Abstract

In this paper we suggest an algorithm for ringing suppression based on a sparse representation method. As one of its steps, the suggested method includes image deblurring based on the Wiener-Hunt deconvolution algorithm. The ringing suppression algorithm uses the signals' mutual coherence and sparsities analysis when dealing with the ringing effect based on the sparse representation method. We also analyze the mutual coherence and sparsities for blurred images and images with white Gaussian noise.

Keywords: RINGING EFFECT, SPARSE REPRESENTATIONS, MUTUAL COHERENCE

Citation: UMN OV AV, KRYLOV AS. RESEARCH OF SPARSE REPRESENTATION METHOD FOR RINGING SUPPRESSION. *COMPUTER OPTICS*, 2016; 40(6): 895-903.

DOI: 10.18287/2412-6179-2016-40-6-895-903.

Introduction

Ringing effect is an artefact that appears as oscillations near strong edges in images. The source of this artifact is high frequency information corruption or loss, and it appears as a result of image processing using various algorithms, in magnetic resonance imaging, and in images transferred through analog channels [1]. The ringing effect is based on the Gibbs phenomenon.

The following algorithms can cause the ringing effect: image deblurring, image super-resolution, image denoising. The most common source of the ringing effect is the image and video compression [2]. An example of image corrupted by ringing effect is shown in fig. 1.



Fig. 1. An example of image corrupted by ringing effect

There are many methods for detection and suppression of the ringing effect caused by JPEG or JPEG 2000 compression algorithms [3-6]. On the other hand, there are only few algorithms that consider the pure ringing effect with various parameters [7-11]. These algorithms are based on the connection between ringing effect and total variation of the image [12, 13], and their main problem is that they do not distinguish between ringing effect and small details in the image, thus the details are corrupted during image processing. One possible method that does not have that problem is given in [14]. In this paper we present a novel algorithm for ringing suppression that produces better results for higher levels of ringing.

In this work the ringing suppression is done using the sparse representations approach that is widely used in signal processing [12, 15], and in image processing [16]. The main idea of this approach is to represent the input data (image patches in our case) as a linear combination of a small amount of signals from the specific redundant dictionary of base signals. The resulting representation is simple and informative at the same time. This approach is described in more detail in section 1.

In section 2 we consider images with different artefacts, such as ringing effect, white Gaussian noise and blur [17], and analyse their mutual coherence and sparsity of their representations. Basing on the results of this analysis we developed a novel method for ringing suppression using sparse representa-

tions, which is described in section 3. The algorithm uses image sharpening with Wiener-Hunt deconvolution algorithm [18] in the learning stage in order to achieve better results.

1. Sparse representations

Let us formulate the sparse representations problem for signals. When applying it to the images we also consider them as one-dimensional signals by concatenating the rows of the image in one-dimensional vector.

Denote the input signal as y , and the dictionary with base signals as matrix D (setting the base signals as columns). Then the representation vector c is found as a solution of the following problem:

$$\min_c \|c\|_0 \text{ subject to } \|y - Dc\|_2 \leq \varepsilon, \quad (1)$$

where $\|c\|_0$ is the number of nonzero coordinates in vector c , and ε is the threshold for the representation error. In general case this problem is NP-hard, but there are algorithms that solve it approximately and give good results in practice [15].

One of such algorithms is Orthogonal Matching Pursuit (OMP). Its main idea is to add elements to the solution support greedily. In each step it chooses such an element so that by adding it to the solution support the approximation of the target vector improves the best. In this work we also tried to use different other algorithms for solving the sparse representation problem, however the OMP algorithm gave the best results. Thus everywhere further we use this algorithm for building sparse representations.

The dictionary in problem (1) can be chosen as a fixed set of signals (for example using discrete cosine transform basis) or by learning the dictionary on the set of signals of the same family as input signals. The second approach usually produces better results, let us examine it in more detail.

Let us denote the set of signals for learning as matrix Y (as columns); the unknown representations of these signals as matrix C (i -th column of the matrix is equal to c_i), and the target dictionary as matrix D . Then the dictionary learning problem can be formulated as:

$$\min_{D,C} \sum_i \|c_i\|_0 \text{ subject to } \|Y - DC\|_2 \leq \varepsilon.$$

There are several approximate algorithms for solving this problem, one of them is the algorithm K-SVD [15]. It uses the idea of alternative itera-

tion optimization: the problem is iteratively solved with respect to representations C using fixed dictionary D and then in turn with respect to dictionary D using fixed representations C . In this work we also tried to use different other algorithms for dictionary learning but the K-SVD algorithm produced the best results. Thus everywhere further we use this algorithm for dictionary learning.

The sparse representation and dictionary learning algorithms require a high amount of calculations, also for the dictionary learning problem a large set of signals for learning is necessary. Thus in order to use this approach for image processing, we split images to the patches of smaller size (we use patches of size 8×8 pixels), and process all the patches independently.

2. Influence of the image artefacts on the sparse representations method

The number of the nonzero coefficients in the representations play important role in the sparse representations method [15]. Let us research how the ringing effect and other artefacts influence this parameter. We consider the blurring of the image and white Gaussian noise along with the ringing artefact. In addition, we research the influence of the image sharpening with Wiener-Hunt deconvolution method, as it is necessary for the development of the suggested ringing suppression method in section 3.

Let us first introduce the concept of mutual coherence for signals in the sparse representations method. We denote as x, y two real vectors, then their mutual coherence is defined as following:

$$\mu(x, y) = \frac{|(x, y)|}{\|x\|_2 \|y\|_2}.$$

If we denote a dictionary with columns d_1, \dots, d_m (the basic signals) as D , then the mutual coherence of this dictionary is defined as [19]:

$$\mu(D) = \max_{i \neq j} \mu(d_i, d_j)$$

In practice the increase of the mutual coherence of a set of signals usually causes the decrease of the number of optimal nonzero coefficients in the representations of the signals in the set. This relation is additionally supported by the fact that in several theorems concerning the sparse representations, the number of nonzero coefficients decreases with the

increase of the dictionary mutual coherence [19]. For example, the uniqueness of the solution c in the problem (1) is guaranteed if the solution satisfies the following property:

$$\|c\|_0 < \frac{1}{2} \left(1 + \frac{1}{\mu(D)} \right).$$

Thus we are going to consider these parameters as reciprocal (and it will be supported by experiments). Next, we give several observations that show that different image artefacts tend to increase or decrease the mutual coherence and present experiments that demonstrate the predicted artefacts influence on the mutual coherence and sparsity.

Let us denote X, Y – independent n -dimensional Gaussian vectors with independent components. Then it can be shown [20], that

$$E(\mu(X, Y)) = \frac{1}{\sqrt{\pi}} \frac{\Gamma(n/2)}{\Gamma((n+1)/2)}.$$

This function is decreasing, thus the increase of the number of independent components n decreases the mutual coherence, and consequently increases the number of nonzero coefficients in representations. The natural images do not precisely fit the model with the independent values of vectors, because the pixels in natural images can be correlated (this usually holds for the neighbor pixels). However, the tendency of sparsity increase with the increase of the number of components still holds true.

Let us first consider the ringing effect. This effect can be modelled using the following procedure. Let us introduce the parameter d and denote as l_d a filter that removes all frequencies outside of the radius $w_d = 1/(2d)$:

$$l_d(w_x, w_y) = \begin{cases} 1, & \text{if } \sqrt{w_x^2 + w_y^2} \leq w_d, \\ 0, & \text{if } \sqrt{w_x^2 + w_y^2} > w_d. \end{cases}$$

With the increase of the parameter d the amount of the removed frequencies also increases, so this parameter corresponds to the ringing strength.

Denoting the discrete cosine transform operator and its inverse as F and F^{-1} correspondingly, let us introduce the ringing effect operator with strength d for image $I(x, y)$:

$$R_d(I) = F^{-1}(l_d \cdot F(I)).$$

This transformation is orthogonal, thus it retains the values of the scalar product and norm and retains vectors independency. In the frequency domain the ringing effect corresponds to the removal of the several of the components, thus using the statement above the mutual coherence must increase, and consequently the sparsity must increase too [20].

The blur effect can be also considered as multiplying the discrete cosine transform coefficients by some filter. For example in the case of Gaussian blur it is a Gaussian function with center in the point that corresponds to the zero frequency. The function greatly decrease the coefficients for some set of frequencies, and completely removes another set of frequencies (after quantization). Thus the number of components decreases, and consequently the mutual coherence and sparsity must increase. On the contrary, if we consider the image sharpening, the mutual coherence and sparsity must decrease.

Let us consider now the noise addition artefact using white Gaussian noise as an example. As it was said before, the natural images do not precisely fit the model with independent components, and this fact increases their mutual coherence comparing to the random vectors. However if we add white noise to the image (the noise is exactly the set of independent components), the correlation between pixels decreases, and the image starts to fit the model with independent components better. Therefore the mutual coherence must decrease, and the number of nonzero coefficients increase.

Let us now demonstrate these observations using numerical experiments. All the experiments were performed using the database [21].

In order to demonstrate the influence of different artefacts on the images mutual coherence we considered random sets of image patches and calculated the average mutual coherence for pairs of patches in the set. For each artefact we considered different values of artefact strength and plotted the dependency between average mutual coherence and the artefact strength. These graphs are shown in fig. 2-4 for ringing effect, blur and noise correspondingly. It can be seen that for the ringing effect and blur the mutual coherence increases with the artefact strength increase, and for the noise it decreases. These results match the observations above. The artefact strength corresponds to the ratio of the removed frequencies for ringing effect, blur strength for image blur and noise amplitude for the noise.

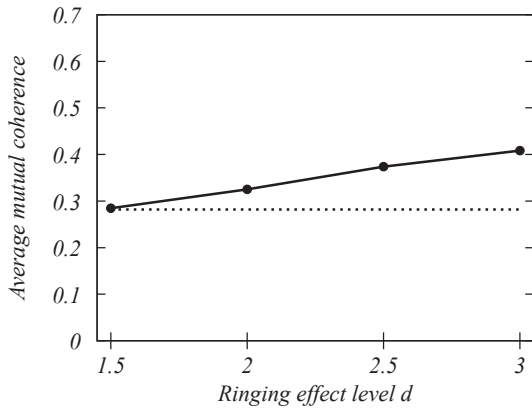


Fig. 2. Influence of the ringing effect on the mutual coherence; dashed line corresponds to the mutual coherence of the natural images and solid line - to the images with different ringing effect levels d

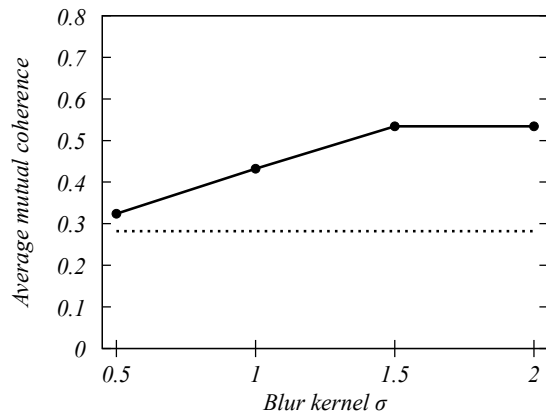


Fig. 3. Influence of the blur effect on the mutual coherence; dashed line corresponds to the mutual coherence of the natural images and solid line - to the images with different blur strengths

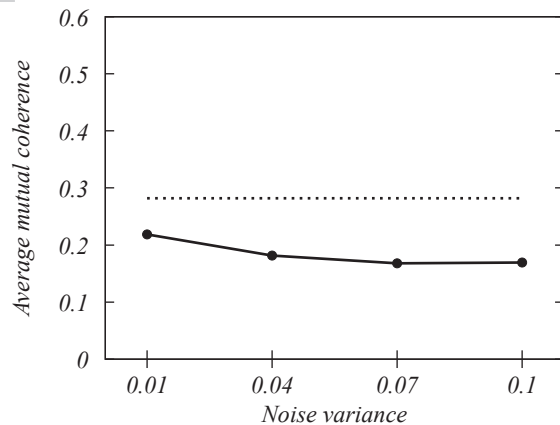


Fig. 4. Influence of the noise addition on the mutual coherence; dashed line corresponds to the mutual coherence of the natural images and solid line - to the images with different levels of noise variance (the pixels intensities take values between 0 and 1)

In order to estimate the best sparsity level for natural images or images with one of the considered artefacts, we learned the dictionary on a set of patches from the considered images and calculated the average sparsity over all representations in the learning set. The obtained value depends not only on the signal type, but also on the error threshold ε . We learned the dictionaries using different values of the threshold and plotted the dependency between the average sparsity and the threshold value. We consider the obtained graph as a characteristic of the sparsity for the artefact and its strength. We give the error values in terms of PSNR metric which is calculated as:

$$PSNR = 10 \log_{10} \left(\frac{MAX_I}{MSE} \right),$$

where MAX_I is the maximum allowed value for the pixels intensity in the image, and MSE is the mean squared error.

Graphs for the error and sparsity dependencies are shown in fig. 5-7. It can be seen that for the ringing and blur effects the number of coefficients increase with the artefact strength increase, and for the noise it decreases, which match the observations above.

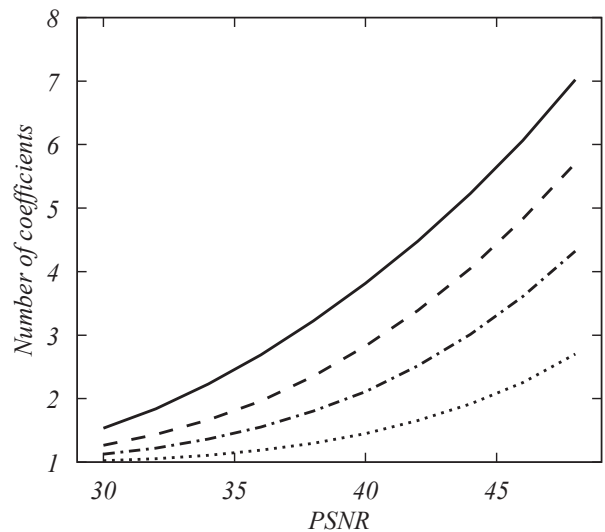


Fig. 5. Influence of the ringing effect on the sparsity; solid line corresponds to the images without artefacts, dashed, dot-dashed and dotted lines correspond to the images corrupted by ringing effect with levels $d=1, 2, 3$ correspondingly

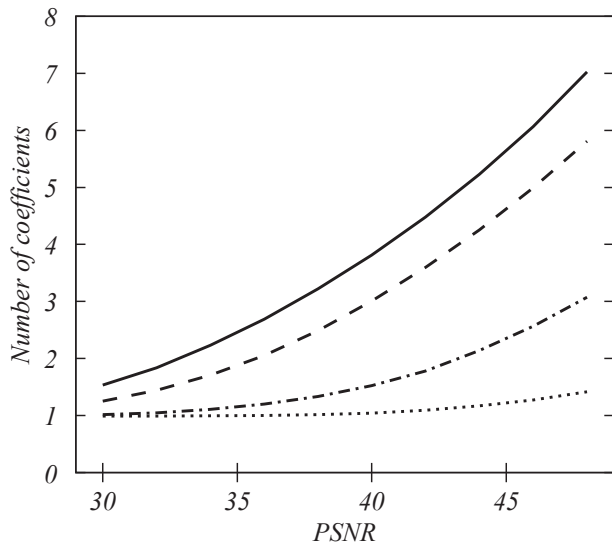


Fig. 6. Influence of the blur effect on the sparsity; solid line corresponds to the images without artefacts, dashed, dot-dashed and dotted lines correspond to the images with blur effect with kernels with $\sigma=0,5, 1, 2$ correspondingly

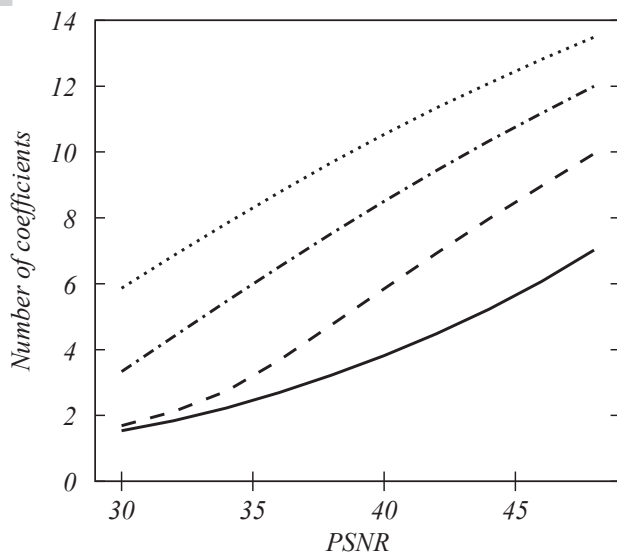


Fig. 7. Influence of the noise addition on the sparsity; solid line corresponds to the images without artefacts, dashed, dot-dashed and dotted lines correspond to the images with noise addition with variances 0,02, 0,05, 0,1 correspondingly

In fig. 8 we also show the graph of the dependency between error and sparsity for the patches of natural images, images with ringing effect and images with ringing effect and sharpening using Wiener-Hunt deconvolution algorithm. It can be seen that the sharpening increases number of necessary nonzero coefficients.

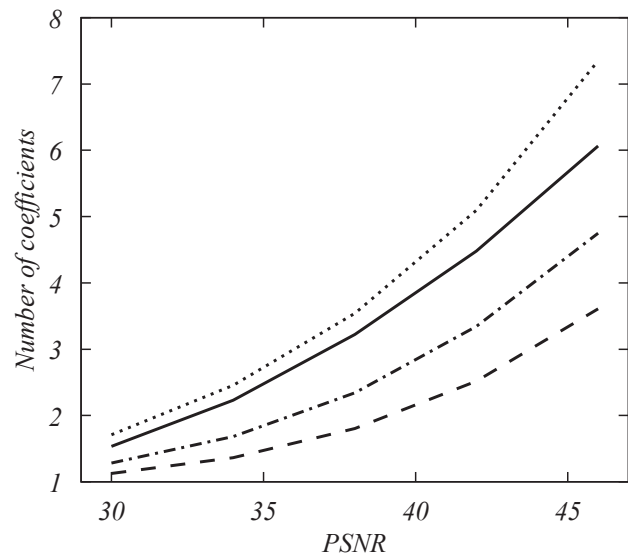


Fig. 8. Influence of the image sharpening on the sparsity; solid line corresponds to the images without artefacts, dashed line corresponds to the images corrupted by ringing effect with level $d = 2$, dot-dashed and dotted lines correspond to the images with ringing effect ($d = 2$) and additional sharpening with Gaussian kernel with σ equal to 1 and 1,5 correspondingly

3. Ringing suppression

In paper [14] we suggested the method for ringing suppression based on sparse representations, and in the learning stage of this method the dictionary was built simultaneously for images with ringing effect and images without it (we denote this method as JC from “joint coding”). In the application stage the method works only with images corrupted by ringing effect, and we found out that optimal sparsity parameters for learning and application greatly differ. We believe that this happens because it is necessary to use different sparsity values for images with ringing effect and images without it (as it was shown in section 2).

Next we present a new algorithm for ringing suppression that is based on the sparse representations method. In this method the dictionaries for natural images and images with ringing effect are learned independently, thus solving the problem described above.

The method uses two learned dictionaries for processing each image patch.

The first dictionary D_1 models the images without ringing effect and is learned on a set of patches from natural images.

The second dictionary D_2 models the pure ringing effect. In order to learn it we use the differences be-

tween images with synthetic ringing effect and corresponding source images.

The ringing effect is the most visible near strong edges in the image. Let us introduce the areas Basic Edges Neighborhood (BEN) and Basic Edges Points (BEP) [1, 9]. These areas are produced by finding the strong edges that are located far enough from other edges (in order to reduce ringing interference). The areas that correspond to the points of the edges are then called BEP and the areas in the close proximity of these points are called BEN. These areas are shown schematically in fig. 9.

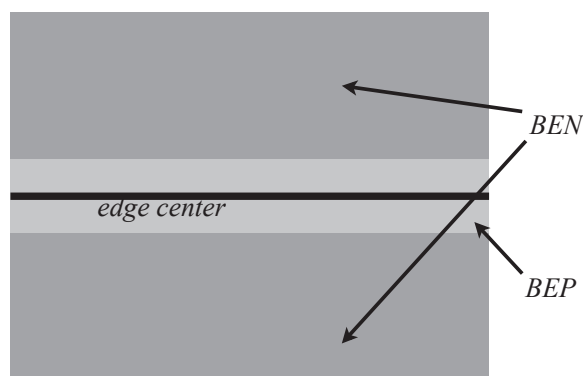


Fig. 9. BEN and BEP areas scheme

In order to improve the quality of the dictionary D_2 we learn it only on the patches in BEN areas as they usually contain the strongest ringing effect oscillations. This condition greatly decreases size of the learning set. However, the ringing effect is invariant to the rotations, thus along with each image in the learning set we can consider its rotated versions as additional examples too. This trick allows us to increase the learning set size. We only used the rotations through angles 90° , 180° and 270° in order to avoid interpolation errors.

Using the two dictionaries D_1 and D_2 described above we create the dictionary $\tilde{D} = [D_1; D_2]$, by uniting their sets of basic signals (columns correspond to the signals). Next for each input image y we find its sparse representation $c = [c_1; c_2]$ using the united dictionary:

$$\min_c \|c\|_0 \text{ subject to } \|y - Dc\|_2 \leq \varepsilon.$$

Then the following holds:

$$Dc = D_1c_1 + D_2c_2.$$

Let us denote the target image without ringing effect as y_1 , then $y = y_1 + y_2$, where y_2 is the image with pure ringing effect. The algorithm that builds the representation c uses basic signals from both dictionaries. The sparsity requirement makes the usage of the basic sig-

nals as efficient as possible. Thus in order to restore the term y_1 the algorithm tends to use mostly signals from D_1 , and in order to restore term y_2 – signals from D_2 . Using this observation we set $y_1 \approx D_1c_1$.

We also found that sharpening of the images with ringing effect while learning the dictionary D_2 increases the method effectiveness. We used Wiener-Hunt deconvolution algorithm for image sharpening. We believe that this improvement is caused by the fact that image sharpening increases the number of coefficients in representations for the dictionary, and thus helps balancing the number of coefficients in the application stage (this leads to the approximately similar sparsity for both dictionaries D_1 and D_2). Additionally the improvement can be caused by the fact that sharpening strengthens the ringing effect in the image, and it helps the learning algorithm better distinguish the ringing effect elements and elements of natural images.

In order to test the method effectiveness we used the images database [21]. We modelled the ringing effect for the images as it was described in section 2, also to make it better correspond to the real ringing effect we added a weak noise to the images. Images were then divided into two groups: for learning and for testing. We measured the method effectiveness by the three following metrics (comparing the restored images and the source images): PSNR calculated globally on the image, PSNR calculated in BEP area and PSNR calculated in BEN area.

The testing was made with different values of the parameter d . We compared the results with the JC method and with method based on the total variation [9] (we denote the method as TV). Comparing the values of the global PSNR we found that for the lower values of parameter $d = 1, 5, 2$ the JC method produces the best results. For the higher values of the parameter $d = 2, 5, 3$ the quality of the JC method and the suggested method are close (results compared to the TV method are similar to those in [14]). The comparison of PSNR values in BEN areas are shown in table 1 and the comparison of PSNR values in BEP areas are shown in table 2.

Table 1. Comparison of the TV method, JC method and the suggested method in terms of PSNR metric values in BEN areas; best values in each row are highlighted with bold font

| d | TV | JC | Suggested |
|-----|-------|--------------|--------------|
| 1.5 | 35.79 | 36.16 | 35.62 |
| 2 | 34.5 | 34.24 | 34.61 |
| 2.5 | 33.62 | 33.05 | 33.65 |
| 3 | 32.64 | 31.36 | 32.78 |

Table 2. Comparison of the TV method, JC method and the suggested method in terms of PSNR metric values in BEP areas; best values in each row are highlighted with bold font

| d | TV | JC | Suggested |
|-----|--------------|-------|--------------|
| 1.5 | 32.29 | 32.27 | 31.45 |
| 2 | 29.12 | 29.04 | 29.26 |
| 2.5 | 26.92 | 26.85 | 27.06 |
| 3 | 25.36 | 25.2 | 25.43 |

The following conclusions can be made. The JC method shows good results in terms of global PSNR for all values of d . However, in the BEN and BEP areas it produces results that are worse than those produced by the TV method and the suggested method. This happens because the JC method is mostly oriented for working with textures, which are not necessarily located near edges. The suggested method shows good results in terms of global PSNR values for higher values of parameter d , and surpasses the results for both TV and JC methods for PSNR value in BEN and BEP areas.

We believe that the suggested method works best for higher values of the parameter d for the following reasons. First, it uses the patches of the bigger size (it was impossible for the JC method to use bigger patches due to the high complexity of the algorithm), and the width of the oscillations and the areas with the strongest ringing effect is growing with the increase of the parameter d . Second, the sparsity difference between normal images and images with ringing effect is more pronounced with higher values of the parameter d (as was shown in the section 2).

A fragment of image corrupted by ringing effect with strength $d = 2.5$ is shown in fig. 10. In fig. 11 we show the same image fragment after suppressing the ringing effect using the JC method, and in fig. 12 – using the suggested method. It can be seen that in some areas near edges the new method works better in removing the artefact oscillations.

The full suggested ringing suppression algorithm is the following. The set of dictionaries for different ringing effect strength values must be learned beforehand. For the input image first the edge blur level σ is detected [1]. In the paper [8] it was shown that the blur level σ depends linearly on the ringing level d . In order to show this the following experiment was made. For a set of edges with different values of the parameter d the best approximation of

the edge using blurred edges was found, and it was shown that the dependency between the blur level σ and ringing level d can be well approximated by the following formula: $\sigma = 0.336d$. Thus after calculating the image blur level σ we can calculate the ringing level as follows: $d = \sigma/0.336$. Using the estimated parameters we then choose the corresponding dictionary and suppress the ringing effect with it.



Fig. 10. Image with the ringing effect ($d = 2.5$) for further ringing suppression



Fig. 11. Image after ringing suppression with JC method ($d = 2.5$)



Fig. 12. Image after ringing suppression with suggested method ($d = 2.5$)

Conclusion

In this paper we analysed the influence of different images artefacts on the number of nonzero coefficients in the sparse representations method. This influence can be formulated as follows: the artefacts that cause image to be less random (i.e. increasing the correlations between pixels) decrease the number of necessary coefficients, and artefacts that cause image to be more random (i.e. decreasing the correlations between pixels) increase the number of necessary coefficients. We presented novel ringing suppression method based on sparse representations. The method was developed using the performed analysis of the influence of the images artefacts on the number of nonzero coefficients in sparse representations. We showed that method outperforms other methods for the images with higher ringing level. The quality increase is the strongest in the areas near image edges.

Acknowledgements

The work was partially funded by the Russian Science Foundation (RSF), grant No. 14-11-00308. For numerical experiments, the Python libraries SciPy [22], Matplotlib [23] and Scikit-learn [24] were used.

References

1. Nasonov AV, Krylov AS. Edge quality metrics for image enhancement. *Pattern Recognition and Image Analysis* 2012; 22(2): 346-353. DOI: 10.1134/S1054661812020113.
2. Koh CC, Mitra SK, Foley JM, Heynderickx I. Annoyance of individual artifacts in MPEG-2 compressed video and their relation to overall annoyance. *Proc SPIE* 2005; 5666: 595-606. DOI: 10.1117/12.587423.
3. Liu H, Klomp N, Heynderickx I. A perceptually relevant approach to ringing region detection. *IEEE Transactions on Image Processing* 2010; 19(6): 1414-1426. DOI: 10.1109/TIP.2010.2041406.
4. Marziliano P, Dufaux S, Winkler T, Ebrahimi T. Perceptual blur and ringing metrics: application to JPEG2000. *Signal Processing: Image Communication* 2005; 19: 163-172. DOI: 10.1016/j.image.2003.08.003.
5. Chang H, Ng MK, Zeng T. Reducing artifacts in JPEG decompression via a learned dictionary. *IEEE Transactions on Signal Processing* 2014; 62(3): 718-728. DOI: 10.1109/TSP.2013.2290508.
6. Shen M-Y, Jay Kuo CC. Review of Postprocessing Techniques for Compression Artifact Removal. *Journal of Visual Communication and Image Representation* 1998; 9(1): 2-14. DOI: 10.1006/jvci.1997.0378.
7. Mosleh A, Langlois JMP, Green P. Image deconvolution ringing artifact detection and removal via psf frequency analysis. *ECCV 2014: Lecture Notes in Computer Science* 2014; 8692: 247-262. DOI: 10.1007/978-3-319-10593-2_17.
8. Umnov A, Nasonov A, Krylov A, Yong D. Sparse method for ringing artifact detection. *ICOSP 2014*: 662-667. DOI: 10.1109/ICO-SP.2014.7015086.
9. Nasonov A, Krylov A. Adaptive image deringing. *Proceedings of GraphiCon 2009*: 151-154.
10. Krylov A, Sitdikov I. Variational image deringing using varying regularization parameter. *Pattern Recognition and Image Analysis* 2015; 25(1): 96-100. DOI: 10.1134/S1054661815010186.
11. Kellner E, Dhital B, Kiselev V, Reiser M. Gibbs-ringing artifact removal based on local subvoxel-shifts. *Magnetic resonance in medicine* 2016; 76(5): 1574-1581. DOI: 10.1002/mrm.26054.
12. Mallat S. *A wavelet tour of signal processing: the sparse way*. Philadelphia: Elsevier; 2009. ISBN: 978-0-12-374370-1.
13. Rudin L, Osher S, Fatemi E. Nonlinear total variation based noise removal algorithms. *Physica D: Nonlinear Phenomena* 1992; 60(1-4): 259-268. DOI: 10.1016/0167-2789(92)90242-F.
14. Umnov A, Krylov A, Nasonov A. Ringing artifact suppression using sparse representation. *ACIVS 2015*: 35-45. DOI: 10.1007/978-3-319-25903-1_4.
15. Elad M. *Sparse and redundant representations*. New York: Springer; 2010. ISBN: 978-1441970107.
16. Elad M, Figueiredo MAT, Ma Y. On the role of the sparse and redundant representations in image processing. *Proc IEEE* 2010; 98(6): 972-982. DOI: 10.1109/JPROC.2009.2037655.
17. Koltsov PP. Image blur estimation. *Computer Optics* 2011; 35(1): 95-102.
18. Orioux F, Giovannelli JF, Rodet T. Bayesian estimation of regularization and point spread function parameters for Wiener-Hunt deconvolution. *JOSA A* 2010; 27(7): 1593-1607. DOI: 10.1364/JOSAA.27.001593.
19. Donoho DL, Elad M, Temlyakov VN. Stable recovery of sparse overcomplete representations in the presence of noise. *IEEE Transactions on Information Theory* 2006; 52(1): 6-18. DOI: 10.1109/TIT.2005.860430.
20. Krylov AS, Umnov AV. Influence of Gibbs phenomenon on the

mutual coherence in sparse representations [In Russian]. Moscow University Bulletin. Series 15: Computational Mathematics and Cybernetics 2016; 4: 12-17.

■ **21.** Ringing analysis database. Source: <http://imaging.cs.msu.ru/research/ringing/database>.

■ **22.** Jones E, Oliphant E, Peterson P, et al. SciPy: Open Source scientific tools for Python. Source: <http://scipy.org>.

■ **23.** Hunter J. Matplotlib: A 2D graphics environment. Computing in Science and Engineering 2007; 9(3): 90-95. DOI: 10.1109/MCSE.2007.55.

■ **24.** Pedregosa F, et al. Scikit-learn: Machine learning in Python. Journal of Machine Learning Research 2011; 12: 2825-2830.

